STEM CELLS AND DEVELOPMENT
Volume 23, Number 5, 2014

DOI: 10.1089/scd.2013.0274

Adult Human Nasal Mesenchymal-Like Stem Cells Restore Cochlear Spiral Ganglion Neurons After Experimental Lesion

Esperanza Bas,[1] Thomas R. Van De Water,[1] Vicente Lumbreras,[2] Suhrud Rajguru,[1,2] Garrett Goss,[1,3] Joshua M. Hare,[3,4] and Bradley J. Goldstein[1,3]

A loss of sensory hair cells or spiral ganglion neurons from the inner ear causes deafness, affecting millions of people. Currently, there is no effective therapy to repair the inner ear sensory structures in humans. Cochlear implantation can restore input, but only if auditory neurons remain intact. Efforts to develop stem cell-based treatments for deafness have demonstrated progress, most notably utilizing embryonic-derived cells. In an effort to bypass limitations of embryonic or induced pluripotent stem cells that may impede the translation to clinical applications, we sought to utilize an alternative cell source. Here, we show that adult human mesenchymal-like stem cells (MSCs) obtained from nasal tissue can repair spiral ganglion loss in experimentally lesioned cochlear cultures from neonatal rats. Stem cells engraft into gentamicin-lesioned organotypic cultures and orchestrate the restoration of the spiral ganglion neuronal population, involving both direct neuronal differentiation and secondary effects on endogenous cells. As a physiologic assay, nasal MSC-derived cells engrafted into lesioned spiral ganglia demonstrate responses to infrared laser stimulus that are consistent with those typical of excitable cells. The addition of a pharmacologic activator of the canonical Wnt/β-catenin pathway concurrent with stem cell treatment promoted robust neuronal differentiation. The availability of an effective adult autologous cell source for inner ear tissue repair should contribute to efforts to translate cell-based strategies to the clinic.

Introduction

Hearing loss affects ~36 million adult humans in the United States. Many forms of sensorineural hearing impairment are due to loss of receptor hair cells and/or spiral ganglion neurons, which carry afferent input from the cochlea. The quest to restore damaged inner ear tissue remains a major challenge. At present, for profound loss that is not helped by hearing-aid amplification, cochlear implantation surgery remains the only treatment option to restore input. However, intact spiral ganglion neurons are required for cochlear implantation or conventional hearing amplification to be useful. Treatment strategies to replace the loss of spiral ganglion neurons are, therefore, needed.

We sought to examine the possibility of utilizing an adult stem cell to treat experimentally lesioned rat cochlear cultures; in principle, an efficacious autologous cell source could translate to clinical use rapidly. We hypothesized that nasal mesenchymal-like stem cells (nasal MSCs) could repair the spiral ganglion, by either directly replacing neurons or via activation of endogenous cells to do so. MSCs from bone marrow have been shown to regulate other stem cell niches while also maintaining a capacity for multilineage differentiation [1,2]. These properties have led to experimental models utilizing various MSCs for tissue repair [2,3]. The nasal MSC is an especially attractive cellular candidate for the repair of neural tissue, because it is an easily obtained autologous source, and the nasal mucosa supports ongoing neurogenesis throughout life to maintain the olfactory neuroepithelium.

The nasal MSC-like cell has been characterized by several groups [4–6]. Importantly, this cell is obtained from the lamina propria, and it differs markedly from the basal cells in the olfactory epithelium, which act as stem cells for the neuroepithelial lineages [7–11]. The precise function of the nasal MSC in the nose remains to be defined; however, these cells are easily cultured from adult human nasal turbinate tissue, while the olfactory basal cells are challenging to propagate from adults. Moreover, nasal MSCs display a transcriptional profile overlapping that of bone marrow MSCs and neural progenitor cells, consistent with their localization within a sensory organ [12]. These properties likely reflect a neural crest origin of mammalian nasal lamina propria cells [13–15], from which the nasal MSCs arise. Nasal

Departments of [1]Otolaryngology and [2]Biomedical Engineering, University of Miami Miller School of Medicine, Miami, Florida.
[3]Interdisciplinary Stem Cell Institute, University of Miami Miller School of Medicine, Miami, Florida.
[4]Cardiovascular Division, Department of Medicine, University of Miami Miller School of Medicine, Miami, Florida.

MSCs have, thus, been tested in models of neural injury, including hippocampal lesions [16], age-related hearing loss [17], and a rat Parkinsonian model [18].

Previous efforts to use various nasal stem cells specifically for auditory repair have shown promise. A mouse nasal neurosphere culture has been demonstrated to have an ability to produce hair cell-like cells under certain culture conditions [19]. However, the origin of the hair cell-like cells may be olfactory epithelial keratin (+) progenitors or lamina propria MSCs, as the nasal neurospheres were prepared from a mixture of both cell types. In addition, using human nasal MSCs in a mouse model of progressive sensorineural deafness, hearing improvement was demonstrated despite a lack of stem cell engraftment, suggesting a beneficial paracrine mechanism of action [17]. These exciting results indicate a need to further define the potential for certain nasal stem cells for inner ear repair. Specifically, conditions promoting stem cell engraftment into damaged inner ear tissue and the possibility for restoration of auditory neurons by nasal stem cells remain to be studied.

More broadly, other sources of stem cells have also demonstrated the principle that a cell-based inner ear therapy is feasible [20,21]. With appropriate induction, a bone marrow MSC can engraft and contribute to auditory neuron repair in certain models [20]. In addition, embryonic stem cells, after precise culture conditions promoted an otic progenitor phenotype, demonstrated remarkable reparative properties when delivered to the gerbil inner ear [21]. Due to potential limitations with other stem cell sources, and the promising characteristics of the nasal stem cells, we focused here on the use of adult human nasal MSCs.

To test our hypothesis, adult human nasal MSCs were obtained, expanded in vitro, and used to treat gentamicin-lesioned postnatal rat organotypic cochlear cultures. Cultures were analyzed by immunochemical staining and confocal microscopy, as well as by voltage-sensitive calcium dye imaging utilizing infrared laser stimulation.

Materials and Methods

Human nasal MSC cultures

Adult human nasal MSCs were prepared as previously described [6,12,22]. Briefly, turbinate tissue was obtained from patients undergoing endoscopic nasal or sinus surgery, following a protocol approved by the Institutional Review Board of the University of Miami. For experiments described here, nasal MSCs obtained from a middle turbinate sample were utilized. Turbinate tissue was held on ice and promptly transported to the lab. Tissue was processed by treatment with dispase II (Roche, Indianapolis, IN) to separate the epithelium from lamina propria. Epithelium was then peeled away and discarded. Lamina propria was then minced, and individual pieces were placed under a glass round cover slip in a 24-well plate with Dulbecco's-modified Eagle's medium (DMEM)/F12 with 10% fetal bovine serum and penicillin (100 U/mL) and streptomycin (100 μg/mL; all from Invitrogen, Grand Island, NY). After adherent cells migrated out and approached confluence, they were treated with trypsin and passaged to culture flasks in the same medium. Cells were then expanded as loosely adherent spheres by seeding $1–5 \times 10^5$ cells per polylysine-coated T25 flask in 5 mL serum-free medium supplemented with fibroblast growth factor 2 (50 ng/mL) and epidermal growth factor (50 ng/mL; both from R&D Systems, Minneapolis, MN) for 3–5 days. Sphere phenotype was assessed by fixing cultures in 4% paraformaldehyde in phosphate buffer solution (PBS), and staining with antibodies to nestin, CD90, CD 105, or Stro1, followed by appropriate fluorescent-conjugated secondary reagents, as previously described [6]. Subsequent experiments were performed using spheres harvested by trituration and brief trysinization, pelleted at 500 *g*, and rinsed in DMEM/F12.

Cochlear cultures

All animal studies were conducted with the approval of the Animal Care and Use Committee of the University of Miami (protocol 11-086) and fully complied with the NIH guidelines for the care and use of laboratory animals. Organ of Corti (OC) explants were harvested from 3 day-old rats. Explants were placed in serum-free media consisting of DMEM supplemented with glucose (final concentration 6 g/L), N-1 supplement (1%), and penicillin G (500 U/mL). OC explants were treated with either gentamicin (10 μM) or PBS vehicle and incubated at 37°C in 95% humidified atmosphere and 5% CO_2. After 4 days, the medium was exchanged for fresh medium (without gentamicin) containing human nasal MSCs; the controls received plain medium without MSCs.

Nasal MSC cochlear treatment

Human nasal MSC spheres at passage 4–6 were labeled with either green fluorescent protein (GFP) or fluorescent nano particles, Qtracker 655 dots (Invitrogen), to permit subsequent detection. For GFP labeling, lentiviral vector encoding GFP (Qiagen, Germantown, MD) was used to transfect the cells, as per the manufacturer's protocol. Briefly, replication-incompetent Cignal GFP control lentiviral particles (catalog number CLS-PCG) were incubated for 24 h with adherent cells at a multiplicity of infection of ~20, with Qiagen SureEntry transduction reagent used at 4 μg/mL. Cells were washed, maintained in normal growth medium for 2 days, and re-seeded in sphere-forming medium before use. Since cells were promptly used for experiments without subsequent passage, puromycin selection was not necessary. For QDot label, sphere-forming cells were harvested, briefly trypsinized to break up spheres, rinsed, and then labeled with Qtracker 655 particles (Invitrogen) as per the manufacturer's instructions. Either GFP-labeled or QDot-labeled sphere-forming cells were centrifuged and washed twice with DMEM/F12, and they were then resuspended in 0.5 mL medium. Approximately 10^5 cells were applied to gentamicin-lesioned cochlear cultures, or control un-lesioned cultures, seeding the cell suspension onto the area of the sensory epithelium in a defined gentamicin-free medium. The medium was changed every 3 days. In a subset of cultures, LiCl (Sigma, St. Louis, MO; 2 mM final concentration) was added to the medium at the time of stem cell treatment, and maintained in subsequent medium changes. Cultures were then analyzed at 10 days post-MSCs treatment.

Immunochemistry and analysis

The tissues were fixed in 4% paraformaldehyde in 0.1 M PBS for 48 h at 4°C. The explants were washed thrice in PBS

and subsequently incubated in 5% normal goat serum, 1% Triton X-100 in PBS for 30 min at 25°C. They were then incubated with Tuj-1 (1:100, MMS-435P; Covance, Princeton, NJ), anti-Synapsin (1:100, 2312; Cell Signaling Technology, Danvers, MA), or anti-Glutamate Receptor 2 and 3 (1:50, AB1506; Millipore, Billerica, MA) in blocking solution at 4°C overnight. After washing, the OC explants were incubated for 90 min at room temperature in blocking solution containing appropriate species-specific fluorescent-conjugated secondary antibodies (Invitrogen). After washing, the explants were counter-stained with 4′,6-diamidino-2-phenylindole (Sigma), washed again, transferred to glass slides with anti-fading mounting medium, and cover slipped. The slides were observed under a Zeiss Axiovert 700 confocal microscope. Image J 1.45h software (NIH, Bethesda, MD) was used for processing and analyzing the images. Cells were considered co-labeled if there was convincing staining with either GFP or QDots in the soma and surrounding immunostaining with appropriate cellular localization on confocal images. For instance, TuJ-1 labels neuron-specific β-tubulin, localizes to the soma, and neurites with a filamentous pattern. By scrolling through z-stacks acquired at 0.5 μm thickness, the accurate distribution and assessment of cell labeling was obtained for purposes of quantification. A region of interest (ROI) of 320×320 μm was used in each case corresponding to the acquired field of vision. ROIs were defined to cover the spiral ganglion region in quantified samples. The investigator was not blinded, as lesioned or unlesioned cultures were markedly different in their staining appearance; however, counts, including ROIs throughout the spiral ganglion regions, were obtained to minimize bias.

Infrared laser stimulation

Multiple studies have highlighted the intracellular calcium $[Ca^{2+}]_i$ responses evoked by pulsed infrared radiation (IR) that result in the activation of spiral and vestibular ganglion neurons, vestibular hair cells, and cardiomyocytes [23–31]. In the present study, pulsed IR and Ca^{2+} imaging was used to test functionality of the cells with a neural fate. We used cochlear explants that were co-cultured with the nasal MSCs. The specimens were loaded and incubated at 37°C for 10 min with 50 μM Ca^{2+}-sensitive dye Fluo-4 AM (Life Technologies, Grand Island, NY) dissolved in dimethylsulfoxide (Sigma) and mixed with 20% Pluronic F-127 (Life Technologies). After incubation, the dye was washed and replaced with artificial perilymph solution (125 mM NaCl; 3.5 mM KCl; 25 mM $NaHCO_3$; 1.2 mM $MgCl_2$; 1.3 mM $CaCl_2$; 0.75 mM NaH_2PO_4; 5 mM glucose). A confocal microscope (SP5 upright; Leica, Wetzlar, Germany) with a resonant scanner was used to image the live human nasal MSC-derived cells labeled with Qtracker 655 particles (red) and the IR-induced changes in $[Ca^{2+}]_i$ measured by the Fluo-4 AM (green). Image sequences (2,56,256 pixels frame^{-1}) with varying IR stimulation parameters were recorded (14 fps). IR stimulation was delivered with a multimodal 400 μm diameter optical fiber (Ocean Optics, Dunedin, FL) that was connected to a Capella laser (Lockheed Martin Aculight, Bothell, WA). The fiber was held and controlled with a micromanipulator, enabling IR to be focused roughly 300–500 μm away from the target cells. A pilot light was used as a guide to position and focus the laser beam onto the cells of interest. The laser source was configured to emit 4 ms pulses with a frequency of 0.5–1 pps using a wavelength of 1,863 nm. The energy output from the fiber, measured in air, was of 1–1.017 mJ. The parameters were chosen based on previous studies that have shown effective and safe stimulation of auditory neurons in vivo [32–34]. Image sequences were processed using ImageJ (NIH) to adjust brightness and contrast. Average fluorescence value of the cells in each frame was computed using an ROI analysis. Here, the ROIs are the areas corresponding to each cell. The QDot positive and negative cells were used as a reference to select ROIs. The normalized fluorescence variations of the cells ($F-F_0/F_0$, where F_0 is the fluorescence intensity value in the first frame of the sequence) stimulated by the pulsed IR were plotted using a custom-written program in MATLAB (MathWorks, Natick, MA).

Statistical analysis

Analysis of variance (ANOVA) followed by Tukey's Multiple-Comparison Test was applied for the engrafted MSC cell study (Fig. 2; $n=6$ independent specimens/group), for the Tuj-1-positive cell quantification (Fig. 4; $n=8$–14 independent specimens/group), and for Tuj-1-positive areas (Fig. 7D; $n=10$ independent specimens/group). To compare the percentage of Tuj-1 positive versus negative LentiGFP human nasal mesenchymal stem cells, an unpaired two-tailed *t*-test was applied (Fig. 6H; $n=6$ independent specimens/group).

Results

Human nasal MSC characterization

The isolation of human nasal MSC-like cells in our lab has been previously reported [6]. The cells used in the present experiments were studied to confirm an appropriate phenotype, before using these cells to treat cochlear cultures. After the processing of adult human lamina propria cells from turbinate tissue and expansion in culture, sphere-forming cells were harvested for passage, discarding the adherent populations, to enrich for nasal MSC-like cells. Cell samples were then characterized immunochemically. Staining results confirm that the sphere-forming cellular phenotype is characterized by the expression of surface proteins which are common to nasal MSC-like cells [6,35], including STRO-1, CD90, CD105, and the intermediate filament nestin (Fig. 1). By fluorescence-activated cell sorting analysis, 100% of nasal MSC sphere cells express CD90 [6]; all sphere-forming cells are nestin (+), although some adherent non-sphere cells do not express nestin (Fig. 1A), and STRO-1 and CD105 expression appears heterogenous. Importantly, cells do not express markers typical of olfactory epithelium, such as cytokeratins, or of hematopoietic lineage, such as CD34 and CD45 (not shown). Human nasal MSCs were labeled with QDot fluorescent nanosphere beads or lentivirus GFP before co-culture experiments, to permit tracking of the cells, and were found to be well labeled (Fig. 1E, F).

Engrafted nasal MSCs migrate to the lesioned spiral ganglion region

Gentamicin treatment is an established technique that is used to experimentally lesion the sensory apparatus of the

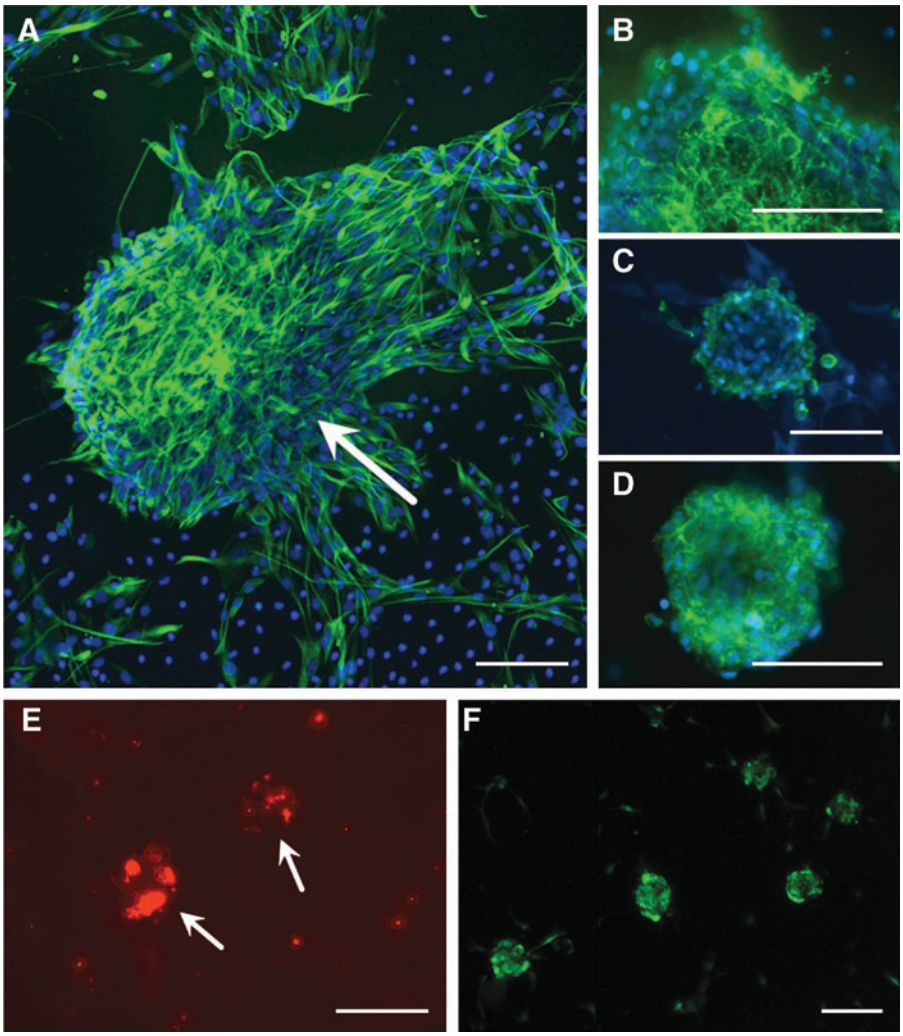

FIG. 1. Human nasal mesenchymal-like stem cells (nasal MSCs) express an appropriate MSC phenotype. **(A)** Under sphere-forming conditions, cells express the intermediate filament Nestin (*green*); *arrow* indicates a large nestin (+) sphere. The surface markers characteristic of MSCs are also expressed, including CD90 **(B)**, CD105 **(C)**, and STRO1 **(D)**. Nuclei are counterstained with 4′,6-diamidino-2-phenylindole (DAPI) (*blue*). **(E, F)** Live nasal MSCs were labeled with either fluorescent nanospheres **(E**, Qtracker 655; Molecular Probes Eugene, OR, USA**)** or green fluorescent protein (GFP) via lentiviral tranfection **(F)** to facilitate tracking cells in a co-culture with rat cochlea. Bar = 50 μm. Color images available online at www.liebertpub.com/scd

inner ear [36–39]. Using this paradigm, we tested the hypothesis that nasal MSC treatment could help repair experimentally lesioned sensory tissue in the cochlea. MSCs are attracted to sites of inflammation or tissue injury [40]. Accordingly, we found that concentrations of labeled nasal MSCs were clustered in the spiral ganglion region of lesioned cultures when stem cells were applied. Cochlear cultures were examined by confocal microscopy, and engrafted stem cell-derived cells were detected by visualization of GFP or fluorescent bead labeling and by immunochemical labeling with Tuj-1 (Fig. 2A–D). No differences were observed between GFP-transfected cells and QDot-labeled cells. Although it is difficult to completely exclude the possibility of rare uptake of QDots by neighboring cochlear cells from dead stem cells, similar findings from GFP- or QDot-labeled experiments strongly suggest that such non-specific labeling is not sufficient to explain our findings. Moreover, QDot passive uptake from either extracellular space or via gap junctions has been carefully studied and previously excluded [41]. Labeled cells were found to localize largely in the spiral ganglion region (Fig. 3). Occasional non-integrated clusters of labeled cells were found attached to cochleae. Rare labeled cells were noted in the OC beneath or adjacent to the hair cell sensory epithelium. However, labeled stem cell-derived hair

FIG. 3. Engrafted nasal MSCs migrate to the spiral ganglion region and promote an increase in spiral ganglion neurons. GM-lesioned cochleae in culture were either untreated **(A)** or treated with nasal MSCs [**(B–D)**, *red*]. An analysis after 14 days shows that cultures which did not receive nasal MSCs have largely absent Tuj-1 neuronal staining in the spiral ganglion **(A)**; in MSC-treated cultures, the nasal MSCs tend to cluster in the lesioned spiral ganglion [**(B)**, *arrows*]; this is readily apparent on orthogonal views in **(B)**, where the Deiter's cells and inner hair cells are identified in the sensorineural epithelia area, and the *red* labeled MSCs engraft in the spiral ganglion area. There are prominent Tuj-1-labeled neuronal processes extending from this region in MSC-treated cultures. Nuclei are counterstained with DAPI (*blue*); bar = 50 μm in Z-stack views and 25 μm in orthogonal views. **(C, D)** A three-dimensional view from a boxed region in **(B) (C)** and a similar region from a different specimen **(D)** show how some neurons with Tuj-1 (+) processes (*green*) are labeled with Qdot beads (*red*), indicating that they are human nasal MSC derived; bar = 5 μm; 40 × oil immersion objective. **(E)** Eosin-stained histologic section through the cochlea, labeled to provide orientation for confocal figures. SGNs, spiral ganglion neurons; IHC, inner hair cell. *Arrowheads* indicate TuJ-1 (+) nasal MSC-derived cells. Color images available online at www.liebertpub.com/scd

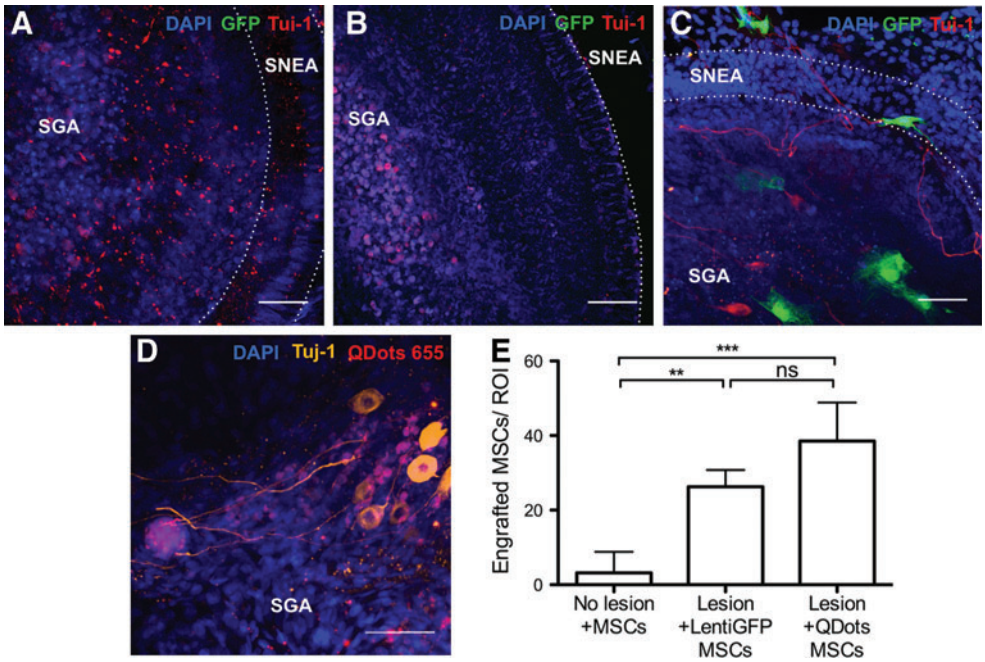

FIG. 2. Human nasal MSCs engraft in lesioned rat cochleae. Co-cultures with lentiGFP-transfected MSCs are shown in **(**A–**C)** (*green*); cultures with QDot 655-labeled MSCs are shown in **(D)** (*red*). The specimens were co-stained with Tuj-1 [*red* in **(A–C)** and *orange* in **(D)**] as a neuron-specific class III beta-tubulin marker and DAPI to visualize nuclei (*blue*). **(A)** Un-lesioned cultures without stem cell treatment show remnants of neurites after a total of 14 days in culture. **(B)** Gentamicin (GM)-lesioned cochlear cultures in which nasal MSCs were not added show absence of neurons and shrunken nuclei. **(C, D)** GM-lesioned explants co-cultured with nasal MSCs show healthy neurons and engrafted nasal MSCs. The sensorineural epithelia area (SNEA) and spiral ganglion area (SGA) are indicated in each photograph. Very few nasal MSCs were identifiable into control, un-lesioned cultures that were stem cell treated **[(E)**, microphotograph not included], indicating that injury or lesion permits stem cell engraftment: 38.5 ± 4.2 QDot-labeled MSCs and 26.2 ± 2.3 LentiGFP-transfected MSCs were identifiable in lesioned cultures; 3.2 ± 2.3 MSCs were identifiable in un-lesioned cultures ($n = 6$ independent specimens/group). Plotted data correspond to the mean ± standard deviation (SD). Analysis of variance (ANOVA) followed by Tukey's test was used for statistics. $^{**}P < 0.05$, $^{***}P < 0.005$, ns, not significant. Bar = 50 μm. Color images available online at www.liebertpub.com/scd

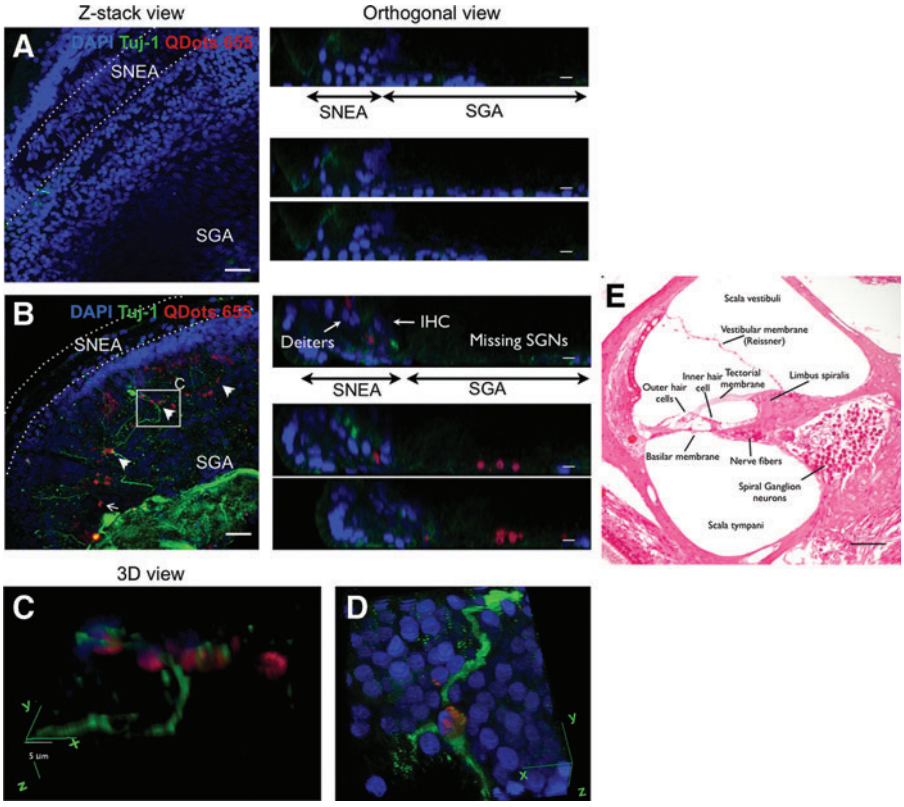

cells were not identified, by position and morphology assessed by orthogonal views on confocal microscopy (Fig. 3B, E). Importantly, little to no nasal MSC engraftment was identified in control un-lesioned cochlear cultures (Fig. 2E). We identified only 3.2 ± 2.3 [standard error of the mean (SEM)] engrafted labeled cells per ROI in control un-lesioned cochlear cultures, after nasal MSC treatment, while we found 38.5 ± 4.2 (SEM) QDot-labeled MSCs and 26.2 ± 2.3 (SEM) LentiGFP-transfected MSCs in lesioned stem cell-treated cultures (Fig. 2E; $n = 6$ independent specimens/group). Therefore, we conclude that tissue injury creates an environment which is permissive to stem cell engraftment and that the different cell labeling methods are equivalent.

Stem cell treatment of lesioned cochleae restores the spiral ganglion neuron population

Lesioned and subsequently stem cell-treated cultures were found to contain numerous spiral ganglion neurons (Fig. 4), in striking contrast to gentamicin-lesioned cochlea cultures that did not receive stem cells (Figs. 2A, B, and 4). Postnatal rat cochlea cultures ($n = 8$) were incubated with medium containing the ototoxic drug gentamicin (10 μM), a well-established technique that causes loss of hair cells as well as subsequent degeneration of spiral ganglion neurons [36,38]. This treatment, as expected, resulted in extensive loss of sensory hair cells and spiral ganglion neurons, when examined 10 days after a 4-day treatment period (Figs. 2–4); at this time point, even the un-lesioned control explants exhibit some degree of degradation of neurites. To test the effect of stem cell treatment, cultures were seeded with nasal MSCs ($n = 14$) or control medium without cells ($n = 8$), and they were analyzed by confocal microscopy with cell type-specific staining after 10 days. Quantification of TuJ-1-labeled neurons indicates a mean of 7.4 ± 4.5 spiral ganglion neurons per field at 4 days after cultures were lesioned with gentamicin. When lesioned cultures were maintained another 10 days but were not stem cell treated, this number dropped to 2.0 ± 1.8. However, in stem cell-treated cochleae, the number of Tuj-1-positive cells was 17.8 ± 5.1, where ~45% were host neurons and 55% were stem cell-derived neurons, based on QDot label (Figs. 2–4). Using lentiGFP-labeled nasal MSCs, 64.4 ± 3.7% of the GFP (+) cells were also Tuj-1 (+) ($n = 5$ independent specimens/group; please also see Fig. 6 graph). These data indicate that adult human nasal stem cell treatment of experimentally lesioned cochlear cultures results in a significant preservation and restoration of spiral ganglion neurons ($P < 0.005$, ANOVA followed by Tukey's Multiple-Comparison Test).

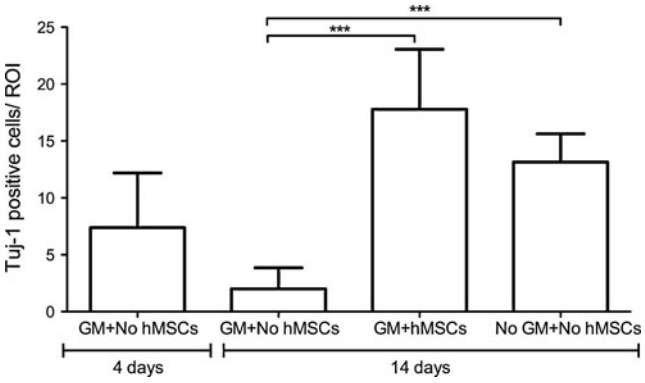

FIG. 4. Human nasal mesenchymal stem cell (hMSC) treatment restores spiral ganglion cell population. Quantification of TuJ-1-expressing neurons in the spiral ganglion from GM-lesioned cultures with no stem cell treatment (GM + No hMSCs), GM-lesioned cultures with human nasal MSC treatment (GM + hMSCs), or un-lesioned cultures (No GM + No hMSCs) indicates that there is an ongoing loss of neurons from 4 to 14 days after GM lesion in cultures not treated with stem cells, and that hMSC treatment results in a restoration of the neuronal population. Mean neuronal counts are markedly increased in GM-lesioned cultures that received hMSCs (17.8 ± 5.1; $n = 14$ cultures) versus GM-lesioned cultures which did not receive hMSCs (2.0 ± 1.8; $n = 8$ cultures, $^{***}P < 0.005$). Plotted data correspond to the mean ± SD. ANOVA followed by Tukey's test was used for statistical analysis.

In the nasal MSC-treated cultures, the spiral ganglion cells labeled with neuron-specific Tuj-1 were noted to bear long neurite-like processes (Figs. 2, 3, and 6). Many of the labeled neurites appear to extend toward the sensory epithelium, and to form synapse-like connections with other cells (Figs. 2, 3, and 6). Although not all MSC-derived TuJ-1 (+) cells had such morphology, we commonly found cells that, when studied by high-resolution confocal Z-stack images, clearly extended labeled neurites to contact other cells, highly suggestive of efforts to establish connections (Fig. 3D).

Spiral ganglion cells in stem cell-treated cultures are excitable

Short pulses of optical IR stimuli ($\lambda = 1{,}863$ nm) have been shown to evoke controllable, pulse-by-pulse $[Ca^{2+}]_i$ transients in the cultured spiral and vestibular ganglion neurons, neurotransmitter release from vestibular hair cells, and contractions in cardiomyocytes [23–26,28–31]. IR stimulation delivered to the QDot-positive cells engrafted in the lesioned spiral ganglion region of neonatal rat cochlear cultures consistently evoked similar, pulse-by-pulse $[Ca^{2+}]_i$ transients, indicating that these cells are excitable ($n = 6$ cochlear cultures, 394 QDot-positive cells analyzed). The evoked changes in $[Ca^{2+}]_i$ by 1 pps optical IR in QDot-positive and -negative cell ROIs are shown in Fig. 5. Before optical stimulation, the extracellular media containing Fluo-4 AM used for incubation was replaced with fresh artificial perilymph. Thus, the measured responses reflected the changes in intracellular Ca^{2+} transients and were not affected by background fluorescence. The responses observed were identical among all cochlear cultures stimulated with IR between 0.5 and 1 pps.

Neurons arise both from engrafted nasal MSCs and from rescue of endogenous cells

Cells in the spiral ganglia of stem cell-treated cultures that express neuronal proteins and have a neuronal morphology were often found to also bear the nasal MSC QDot label (Fig. 3). In experiments using a lenti-GFP technique to label MSCs, similar labeling patterns and results were also obtained, confirming the utility of the QDot marker (Figs. 2 and 6). Many of these MSC-derived cells have a neuronal morphology, are labeled by the neuron-specific marker TuJ-1, and appear to extend neurite-like processes toward other cells, often toward the sensory epithelium (Figs. 3 and 6). The

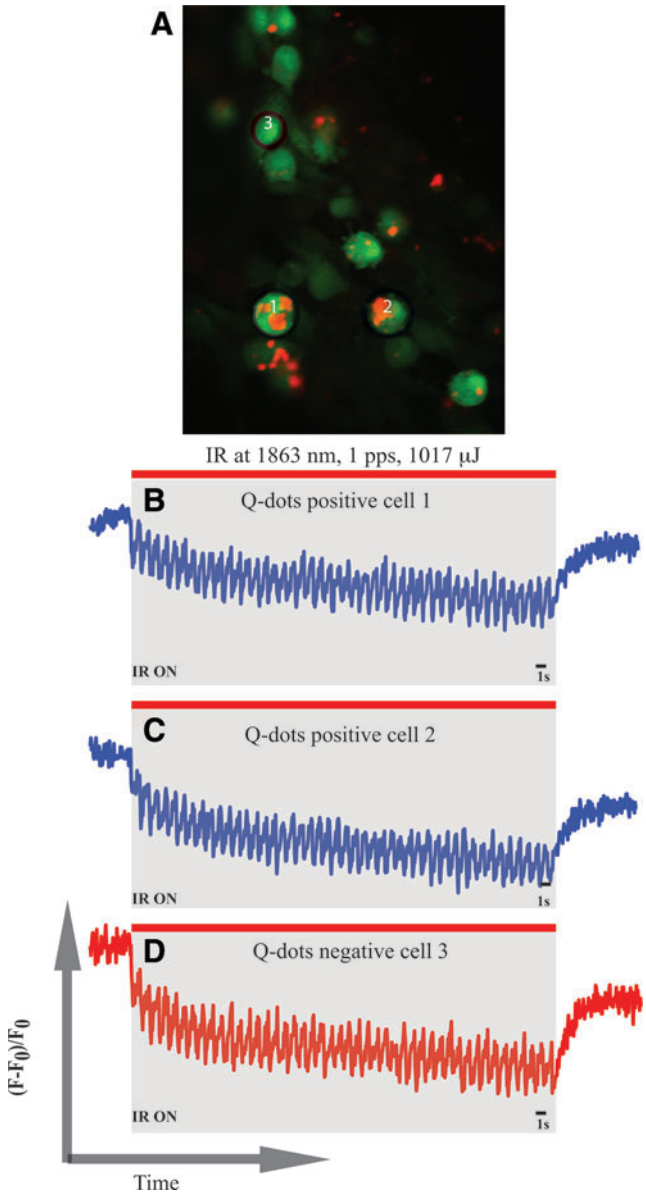

FIG. 5. MSC-derived cells display excitable responses to infrared laser stimulus. **(A)** Shows QDot-positive and -negative cells after loading with Ca^{2+}-sensitive dye Fluo-4 AM. Two QDot-positive (ie, nasal MSC-derived) cells and one QDot-negative cell were selected to analyze their responses to infrared radiation (IR) stimulation for 1 min at 1,893 nm, 1 pps, and 1,017 mJ of radiant energy. Normalized fluorescence values were plotted over time. Traces **(B)** and **(C)** show the IR-evoked $[Ca^{2+}]_i$ transients in the two selected QDot-positive cells. Trace **(D)** shows the response of a QDot-negative endogenous cell, which can be a spiral ganglion neuron or a glial cell. Responses obtained in traces **(B–D)** are similar to the ones obtained in excitable cells such as neurons or cardiomyocytes. Color images available online at www.liebertpub.com/scd

efficiency of the QDot label is estimated to be in the 50% range, based on an examination of nasal MSCs in vitro (Fig. 1). Although mitoses can dilute the nanoparticle concentration in cells, we have found that the label remains fluorescently detectable despite proliferation, as have other investigators [41]. Nonetheless, not all spiral ganglion neurons in our stem cell-treated cultures are co-labeled by the fluorescent QDot marker. Approximately 45% of spiral ganglion neurons in MSC-treated cultures were not clearly bead labeled, but were generally seen in areas with surrounding labeled MSC-derived cells. These data strongly suggest that an important mechanism by which adult nasal MSCs repair the spiral ganglion is by a paracrine-type effect on endogenous spiral ganglion cells, in addition to a capacity to directly differentiate into new neurons.

Indeed, the morphology of non-bead-labeled (ie, endogenous) neurons in the spiral ganglia of nasal MSC-treated cultures was different from many QDot-labeled or GFP-labeled neurons. These endogenous neurons have large, round cell bodies, typical of spiral ganglion neurons seen in unlesioned control cultures (Fig. 2D). That large, round, QDot (−) TuJ-1 (+) cells are essentially absent from gentamicin lesioned cultures which were not stem cell treated, and are found in stem cell-treated cultures in areas with surrounding bead-labeled cells, suggests a paracrine mechanism of action by which nasal MSCs are promoting the survival of endogenous cells. Neurons were not labeled by the S-phase mitotic marker 5-bromodeoxyuridine (BrdU, not shown), when BrdU was maintained in medium from the time of stem cell addition. Since nasal MSC-driven neurogenesis does not appear to be a proliferative regeneration, we conclude that stem cells are promoting the survival of endogenous neurons in gentamicin-lesioned cultures, although we cannot exclude the possibility of the differentiation of neurons from other precursor cells, to account for the numbers of Tuj-1 (+) cells identified at 10 days after stem cell treatment (Fig. 4). We conclude from these data that both survival promotion and the differentiation of neurons from MSCs are contributory.

Spiral ganglion neurons in stem cell-treated cultures exhibit evidence of appropriate differentiation, enhanced by activation of Wnt/β-catenin signaling

To further characterize neuronal cells in nasal MSC-treated cultures, samples were probed for expression of synapsin and glutamate receptors (Figs. 6 and 7). Synapsins are a family of phosphoproteins; types I and II are localized mainly in minor processes and in axons, while type III has been found in the cell bodies, axons, and growth cones in developing neurons [42,43]. The antibody used here recognizes all three forms of synapsins and, therefore, labels the cell somata in many of our images. Glutamate receptor is a neurotransmitter receptor that is expressed in the spiral ganglion and sensory neuroepithelium [44,45]. Lesioned controls, not treated with stem cells, again exhibited almost no neurons and minimal synapsin labeling (Fig. 6C, D). Stem cell-treated cultures had, in contrast, robust clusters of TuJ-1 (+) neurons with large, round cell bodies, with synapsin expression overlapping their cell bodies and neurites (Fig. 6E–G), such as the spiral ganglia neurons of the 1 day post-explant un-lesioned control group (Fig. 6A, B).

Wnt signaling has been shown to promote olfactory stem cell neurogenesis [46], and it has broad roles in neuronal development, stem cell niche maintenance, and synapse assembly [47,48]. Moreover, Wnt/β-catenin activation enhances neurogenic gene activation in bone marrow MSCs [20]. Accordingly, we examined a role for Wnt pathway activation in the promotion of neurogenesis in the stem cell-

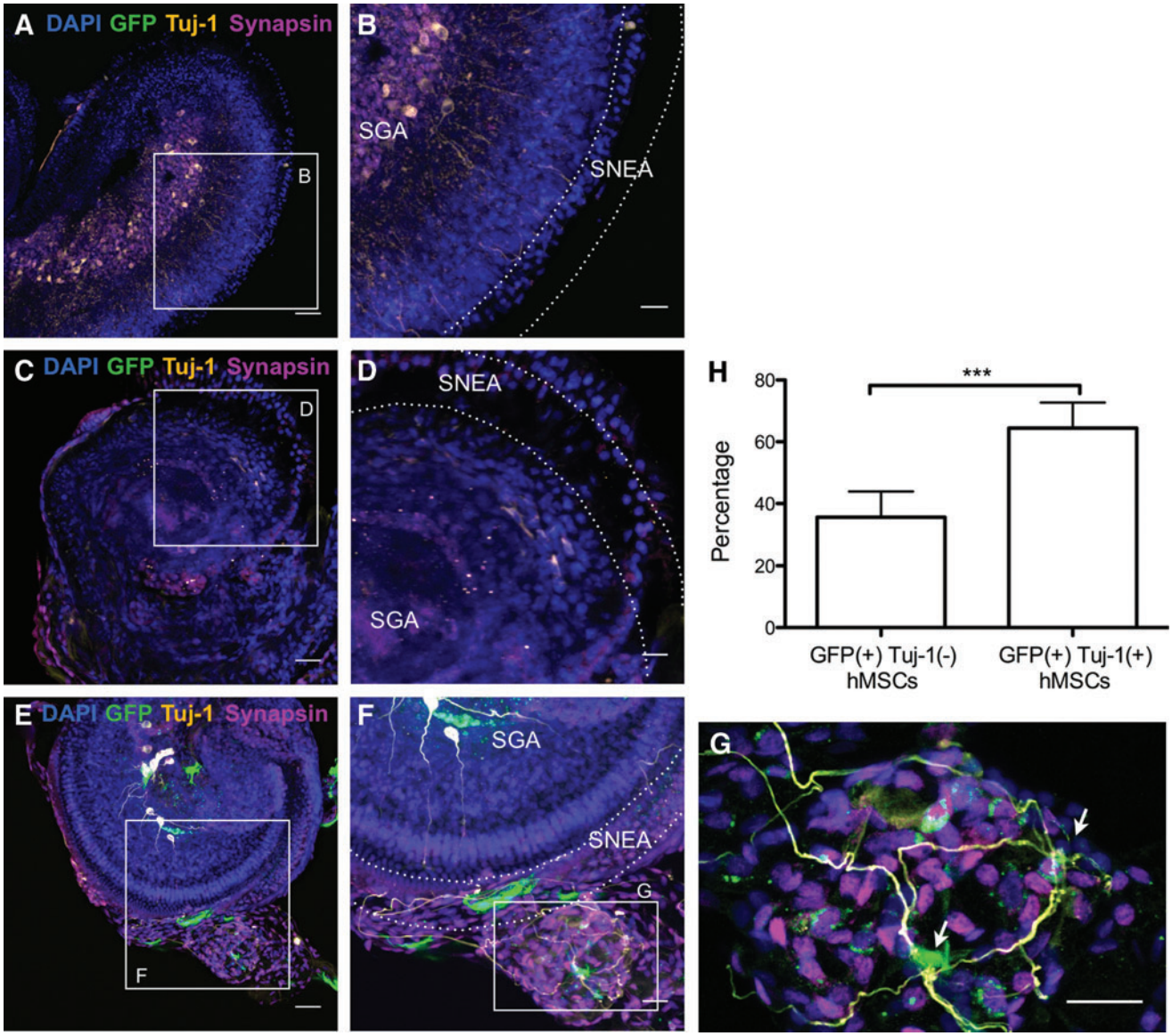

FIG. 6. Differentiation of spiral ganglion neurons in human nasal MSC-treated cochlear cultures. **(A, B)** Un-lesioned control at 1 day post-explantation shows extensive synapsin (*magenta*) and Tuj-1 (*orange*) labeling. **(C, D)** Neuron-specific Tuj-1 labeling and synapsin staining is absent in GM-lesioned cochlea without stem cell treatment. **(E–G)** GM-lesioned stem cell-treated cultures exhibit robust Tuj-1 labeling (*orange*) of neurons and synapsin labeling (*magenta*) among lentiGFP-transfected nasal MSCs (*green*); SNEA and SGA are indicated in the figures. A cluster of ectopically-located nasal MSC-derived cells is visible in this field **(G)**, with extensive synapsin expression and several prominent TuJ-1 (+) processes extending toward the sensory epithelium. *Arrows* indicate GFP (+)/TuJ-1 (+) cells. **(A, C, E)** Bar = 50 μm. **(B, D, F, G)** Bar = 25 μm. **(H)** Graph showing the percentage of GFP-labeled MSCs that are positive and negative for Tuj-1 staining. Plotted data correspond to mean ± SD. Unpaired two-tailed *t*-test was applied ($n = 6$ independent specimens/group, $^{***}P < 0.001$). Color images available online at www.liebertpub.com/scd

treated cochlea. When cultures were treated with addition of the canonical Wnt pathway activator LiCl [49], the density, branching, and complexity of dendritic processes were grossly increased (Fig. 7). We quantified the area of TuJ-1-labeled neurites, indicating 33,679 ± 7,432 μm^2 labeled in the presence of LiCl versus 3,629 ± 596 μm^2 without LiCl ($n = 10$; $P < 0.001$, ANOVA), in stem cell-treated cultures (Fig. 7D). LiCl alone did not have a significant effect. Moreover, intense expression of the neurotransmitter receptors GluR2/R3 was immunochemically identifiable in the stem cell-treated cultures in which LiCl was added (Fig. 7). Taken together, these data indicate that neuronal differentiation occurs in nasal MSC-treated cochlear cultures after gentamicin lesion. In addition, modulation of the Wnt/β-catenin signaling pathway promotes nasal MSC-activated cochlear neurogenesis.

Discussion

We demonstrate here for the first time that a nasal stem cell harvested from adult humans is efficacious in the repair of spiral ganglion neuron loss in experimentally lesioned cochlea. Efforts to develop a cell-based therapy for deafness have recently witnessed significant advances [21,50,51]. These breakthroughs have demonstrated the ability to

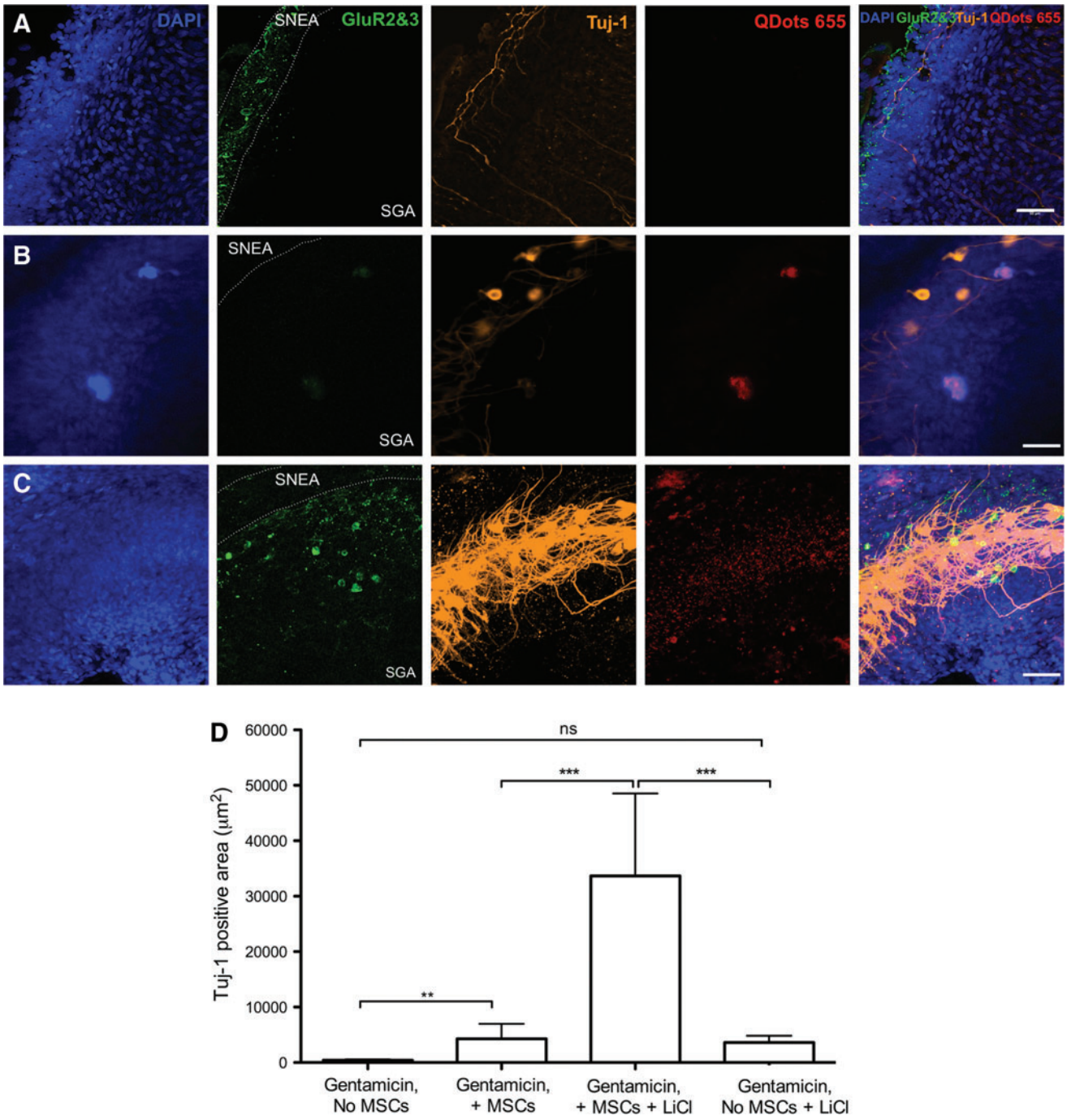

FIG. 7. Pharmacologic activation of Wnt signaling pathway alters the neurite morphology in stem cell-treated cultures at 14 days. **(A)** Control un-lesioned cultures show typical Tuj-1 labeling, along with low levels of glutamate receptor GluR2/3 when maintained in vitro for 14 days. **(B)** In GM-lesioned cultures treated with human nasal MSCs alone, both TuJ-1 (+) neurons (*orange*) and faint GluR2/3 staining (*green*) are evident. **(C)** In GM-lesioned cultures treated with stem cells and LiCl (a Wnt/β-catenin pathway activator), TuJ-1 (+) cells exhibit pronounced density of staining and dendritic arborization (*orange* label, *middle column*); GluR2/3 staining is also more robust (*green*) in adjacent areas; SNEA and SGA are labeled; bar = 50 μm. **(D)** Measurement of the TuJ-1 labeled area, which labels neurites, indicates a significant increase in stem cell-treated cultures that are maintained with LiCl. The TuJ-1 label reflects the increased complexity and density of neurite outgrowth. $^{**}P < 0.05$, $^{***}P < 0.005$, ns, not significant. Color images available online at www.liebertpub.com/scd

generate replacement cells for inner ear sensory structures, including hair cells and spiral ganglion neurons. However, a major limitation is that many of these techniques required the use of either embryonic stem cells or induced pluripotent stem cells. Given the inherent ethical or safety concerns with the use of these cell types, an effective autologous adult cell source offers advantages in terms of efforts to translate these techniques into clinical trials.

What are the properties of MSCs in general, and nasal MSC-like cells in particular, enabling these cells to repair

tissue? The best-characterized MSC is, by far, the bone marrow MSC [52]. Utilizing both autologous and allogeneic bone marrow MSCs to repair damaged tissue in other organs in human clinical trials has shown promising results in terms of safety and efficacy [53]. Mechanistically, MSCs have properties that make them ideal candidates for use in regenerative medicine: they can home to sites of tissue injury or inflammation, communicate with epithelial cells and inflammatory cells, appear to regulate other stem cell niches, and maintain the ability for multilineage differentiation [1–3,40]. Multiple lines of evidence have shown a reparative potential for nasal MSCs in the brain [16,18] and, at least, via a paracrine effect, in a mouse hair cell degeneration model [17]. The results presented here extend these studies to demonstrate an ability of adult human nasal MSCs to dramatically restore the spiral ganglion population of the experimentally lesioned cochlea in vitro.

Two previous studies have reported efforts to use nasal-derived stem cells to repair inner ear tissues [17,19]. It is of interest to discuss our new findings with regard to the earlier data. Among the most critical factors to be considered when comparing results is the type of stem cells utilized, because olfactory mucosa contains multiple types of stem and progenitor cells, with differing growth characteristics and differentiation capacities [8,35]. Potential progenitor or sphere-forming cells may arise from the lamina propria (MSCs, glial cells, and hematopoietic cells) or from olfactory epithelium (horizontal basal cells, globose basal cells). In addition, human and rodent olfactory cultures may not necessarily give rise to progenitors with identical growth characteristics. Barnett and colleagues have described in great detail that spheres can arise from both olfactory epithelium and lamina propria cells, at least when propagated from embryonic rodent tissue [35].

In terms of previous reports using nasal stem cells for cochlear repair, Doyle et al. describe the significant achievement of the production of sensory hair cells from mouse nasal stem cells [19]. However, in the results reported here using human cells, we did not find new hair cell production, likely explained by differences in nasal cell types utilized. The spheres described by Doyle et al. [19] contained cells derived from the olfactory epithelium, rather than purely the lamina propria, evidenced by the expression of cytokeratins. In olfactory tissue, cytokeratins 5 and 14 are specifically expressed by horizontal basal cells in olfactory mucosa, and they are not produced by nasal MSCs from the lamina propria. In addition, their spheres contained cells expressing the transcription factor Pax 6. Pax 6 is expressed by several olfactory cell types, including horizontal basal cells, sustentacular cells, a subset of globose basal cells, and rare Bowman's gland acinar cells [54,55]. Their culture technique prepared olfactory cells from mice and included a mixture of epithelium and lamina propria; thus their neurospheres comprised a mixture of both olfactory epithelial-derived basal cells and lamina propria-derived MSCs. Using these neurospheres, the investigators altered culture conditions to induce the differentiation of a small percentage of nasal-derived cells into a hair cell-like phenotype. We found no evidence of new hair cells produced from our nasal MSCs. In fact, we found that nasal MSC-derived cells were generally not found in the sensory epithelium when engrafted into rat cochlea cultures. Our technique utilized adult human turbinate tissue and carefully excluded the epithelium, in an effort to propagate nasal MSCs. It will be of interest to determine whether human nasal cytokeratin (+) spheres might have a capacity to produce hair cells under certain conditions.

In another report, nasal-derived cells were used to treat progressive sensorineural hearing loss in a mouse model [17]. In that work, the investigators used a human nasal MSC, likely quite similar to the cells we have utilized. The mouse model exhibits a progressive loss of hair cells, causing hearing decline. Interestingly, the treatment of this mouse model with nasal MSCs improved hearing, but the cells did not engraft into the OC sensory epithelium. This is in agreement with our results, in which we found MSC engraftment in the damaged spiral ganglion region, but rarely in the sensory epithelium. In addition, their findings were interpreted as evidence of a paracrine effect from MSCs, which is consistent with the rescue or induction of endogenous spiral ganglion neurons noted in our results, likely via paracrine mechanisms. It is possible that future experiments using alternate delivery techniques or the use of specific induction agents may promote cell engraftment in the hair cell epithelium.

Our results demonstrate several key findings regarding nasal MSC cochlear treatment. Importantly, the nasal MSCs engrafted into the explant. As discussed, engrafted cells localized preferentially to the damaged spiral ganglion region, and we found a large increase in spiral ganglion neuronal numbers after stem cell treatment, which involved both direct differentiation of nasal MSCs into neurons and secondary effects on endogenous cells. Our data provide evidence that nasal MSCs stimulate secondary endogenous responses, leading to spiral ganglion survival or replacement, consistent with observations on the effects of nasal MSCs on neurogenesis in other systems such as the hippocampus [16]. Such secondary effects from engrafted MSCs have also been demonstrated in careful analyses of experiments in which bone marrow MSCs were used to treat experimentally induced cardiac injury in pigs [3]. In those experiments, along with a small number of cardiomyocytes emerging directly from MSCs, MSC–host cell interactions led to activation of a population of endogenous progenitors and subsequent tissue repair.

Our results also revealed that the responses to optical IR stimulation of differentiated MSCs engrafted in the cochlea were similar to those elicited by spiral ganglion neurons. Previous experiments have shown similar responses in excitable cells [23–26,28–31]. This suggests that engrafted MSC-derived cells are, indeed, excitable and may be functionally similar to spiral ganglion neurons. It will be of importance, in future experiments, to focus on further electrophysiological characterization of these cells. Other data have shown that specific electrophysiological features differ between neurons which innervate the high- and low-frequency regions [56]. Whether the differentiated MSCs replicate these characteristics remains to be investigated.

The overall reparative effects of nasal MSC treatment, as evidenced by neurotubulin labeling in the spiral ganglia, were enhanced by the addition of lithium chloride to cultures as a conditioning agent. Lithium chloride is a pharmacologic activator of the Wnt/β-catenin pathway. In spiral ganglion neurons, lithium selectively promotes the phases of neuritogenesis that are associated with microtubule

reorganization, such as sprouting and branching of neurites [49]. Manipulation of this signaling pathway was chosen, because MSCs from bone marrow can be induced toward neuronal differentiation by β-catenin activation, which drives the production of basic helix-loop-helix neurogenic transcription factors, including Ascl1 (Mash1), Neurogenin, and NeuroD [20]. Our MSCs are obtained from nasal mucosa, and in olfactory tissue, Wnt/β-catenin signaling promotes neurogenesis through activation of olfactory epithelial basal cells [46]. Moreover, engraftment of bone marrow MSCs in the gerbil inner ear is increased on pre-induction of the cells with Wnt1, likely due to induction of the neurogenic transcription factors [20]. Ultimately, successful clinical implementation of stem cell inner ear therapies will benefit from optimal conditioning of the cells, and lithium chloride is a pharmacologic agent already in clinical use, making this an attractive conditioning candidate.

Hypotheses regarding the regenerative effects of MSCs have been a subject of debate. A number of paracrine and autocrine mechanisms likely contribute to tissue repair. Our results are consistent with a model in which nasal MSCs likely modulate multiple reparative actions after gentamicin-induced cochlear damage. Future steps toward the implementation of translational experiments will include intact animal experiments with nasal MSCs, utilizing recently proven cellular delivery methods to the cochlea [20,21,57]. Our demonstration of the ability of an easily obtained and autologously available adult human stem cell to repair auditory neuron loss should enhance progress toward the establishment of cell-based therapies for certain forms of deafness.

Acknowledgments

The authors thank members of the Interdisciplinary Stem Cell Institute at the University of Miami Miller School of Medicine for their advice and support. The infrared stimulation work was supported by NIH/NIDCD R01DC011481-02A2 (S.R.).

Author Disclosure Statement

T.R.V. and E.B. have funding from MED-EL Hearing Implants Corporation.

References

1. Pittenger MF. (1999). Multilineage potential of adult human mesenchymal stem cells. Science 284:143–147.
2. Williams AR and JM Hare. (2011). Mesenchymal stem cells: biology, pathophysiology, translational findings, and therapeutic implications for cardiac disease. Circ Res 109:923–940.
3. Hatzistergos KE, H Quevedo, BN Oskouei, Q Hu, GS Feigenbaum, IS Margitich, R Mazhari, AJ Boyle, JP Zambrano, et al. (2010). Bone marrow mesenchymal stem cells stimulate cardiac stem cell proliferation and differentiation. Circ Res 107:913–922.
4. Murrell W, F Feron, A Wetzig, N Cameron, K Splatt, B Bellette, J Bianco, C Perry, G Lee and A Mackay-Sim. (2005). Multipotent stem cells from adult olfactory mucosa. Dev Dyn 233:496–515.
5. Jakob M, H Hemeda, S Janeschik, F Bootz, N Rotter, S Lang and S Brandau. (2010). Human nasal mucosa contains tissue-resident immunologically responsive mesenchymal stromal cells. Stem Cells Dev 19:635–644.
6. Goldstein BJ, JM Hare, S Lieberman and R Casiano. (2013). Adult human nasal mesenchymal stem cells have an unexpected broad anatomic distribution. Int Forum Allergy Rhinol 3:550–555.
7. Calof AL and DM Chikaraishi. (1989). Analysis of neurogenesis in a mammalian neuroepithelium: proliferation and differentiation of an olfactory neuron precursor *in vitro*. Neuron 3:115–127.
8. Huard JM, SL Youngentob, BJ Goldstein, MB Luskin and JE Schwob. (1998). Adult olfactory epithelium contains multipotent progenitors that give rise to neurons and non-neural cells. J Comp Neurol 400:469–486.
9. Goldstein BJ, H Fang, SL Youngentob and JE Schwob. (1998). Transplantation of multipotent progenitors from the adult olfactory epithelium. Neuroreport 9:1611–1617.
10. Leung CT, PA Coulombe and RR Reed. (2007). Contribution of olfactory neural stem cells to tissue maintenance and regeneration. Nat Neurosci 10:720–726.
11. Fletcher RB, MS Prasol, J Estrada, A Baudhuin, K Vranizan, YG Choi and J Ngai. (2011). p63 regulates olfactory stem cell self-renewal and differentiation. Neuron 72:748–759.
12. Delorme B, E Nivet, J Gaillard, T Haupl, J Ringe, A Deveze, J Magnan, J Sohier, M Khrestchatisky, et al. (2010). The human nose harbors a niche of olfactory ectomesenchymal stem cells displaying neurogenic and osteogenic properties. Stem Cells Dev 19:853–866.
13. Katoh H, S Shibata, K Fukuda, M Sato, E Satoh, N Nagoshi, T Minematsu, Y Matsuzaki, C Akazawa, et al. (2011). The dual origin of the peripheral olfactory system: placode and neural crest. Mol Brain 4:34.
14. Forni PE, C Taylor-Burds, VS Melvin, T Williams and S Wray. (2011). Neural crest and ectodermal cells intermix in the nasal placode to give rise to GnRH-1 neurons, sensory neurons, and olfactory ensheathing cells. J Neurosci 31:6915–6927.
15. Forni PE and S Wray. (2012). Neural crest and olfactory system: new prospective. Mol Neurobiol 46:349–360.
16. Nivet E, M Vignes, SD Girard, C Pierrisnard, N Baril, A Deveze, J Magnan, F Lante, M Khrestchatisky, F Feron and FS Roman. (2011). Engraftment of human nasal olfactory stem cells restores neuroplasticity in mice with hippocampal lesions. J Clin Invest 121:2808–2820.
17. Pandit SR, JM Sullivan, V Egger, AA Borecki and S Oleskevich. (2011). Functional effects of adult human olfactory stem cells on early-onset sensorineural hearing loss. Stem Cells 29:670–677.
18. Murrell W, A Wetzig, M Donnellan, F Feron, T Burne, A Meedeniya, J Kesby, J Bianco, C Perry, P Silburn and A Mackay-Sim. (2008). Olfactory mucosa is a potential source for autologous stem cell therapy for Parkinson's disease. Stem Cells 26:2183–2192.
19. Doyle KL, A Kazda, Y Hort, SM McKay and S Oleskevich. (2007). Differentiation of adult mouse olfactory precursor cells into hair cells *in vitro*. Stem Cells 25:621–627.
20. Kondo T, AJ Matsuoka, A Shimomura, KR Koehler, RJ Chan, JM Miller, EF Srour and E Hashino. (2011). Wnt signaling promotes neuronal differentiation from mesenchymal stem cells through activation of Tlx3. Stem Cells 29:836–846.
21. Chen W, N Jongkamonwiwat, L Abbas, SJ Eshtan, SL Johnson, S Kuhn, M Milo, JK Thurlow, PW Andrews, et al. (2012). Restoration of auditory evoked responses by human ES-cell-derived otic progenitors. Nature 490:278–282.

22. Girard SD, A Deveze, E Nivet, B Gepner, FS Roman and F Feron. (2011). Isolating nasal olfactory stem cells from rodents or humans. J Vis Exp pii: 2762.
23. Dittami GM, SM Rajguru, RA Lasher, RW Hitchcock and RD Rabbitt. (2011). Intracellular calcium transients evoked by pulsed infrared radiation in neonatal cardiomyocytes. J Physiol 589:1295–1306.
24. Izzo AD, JT Walsh, Jr., H Ralph, J Webb, M Bendett, J Wells and CP Richter. (2008). Laser stimulation of auditory neurons: effect of shorter pulse duration and penetration depth. Biophys J 94:3159–3166.
25. Jenkins MW, AR Duke, S Gu, HJ Chiel, H Fujioka, M Watanabe, ED Jansen and AM Rollins. (2010). Optical pacing of the embryonic heart. Nat Photonics 4:623–626.
26. Rajguru SM, CP Richter, AI Matic, GR Holstein, SM Highstein, GM Dittami and RD Rabbitt. (2011). Infrared photostimulation of the crista ampullaris. J Physiol 589:1283–1294.
27. Richter CP, R Bayon, AD Izzo, M Otting, E Suh, S Goyal, J Hotaling and JT Walsh, Jr. (2008). Optical stimulation of auditory neurons: effects of acute and chronic deafening. Hear Res 242:42–51.
28. Smith NI, Y Kumamoto, S Iwanaga, J Ando, K Fujita and S Kawata. (2008). A femtosecond laser pacemaker for heart muscle cells. Opt Express 16:8604–8616.
29. Greenberg J, S Rjaguru, D Pelaez and H Cheung. (2013). Pulsed Infrared Radiation leads to synchronous contraction in stem cell derived cardiomyocytes. In: *29th Southern Biomedical Engineering Conference.* Diaz JR, R Jung and A McGoron, eds. Proceedings of the IEEE EMBS, Miami, FL.
30. Lumbreras V, B Esperenza, C Gupta and SM Rajguru. (2013). Pulsed infrared-evoked intracellular calcium transients in neonatal vestibular and spiral ganglion neurons. In: *29th Southern Biomedical Engineering Conference.* Diaz JR, R Jung and A McGoron, eds. Proceedings of the IEEE EMBS, Miami, FL.
31. Richter CP, AI Matic, JD Wells, ED Jansen and JT Walsh, Jr. (2011). Neural stimulation with optical radiation. Laser Photon Rev 5:68–80.
32. Goyal V, S Rajguru, AI Matic, SR Stock and CP Richter. (2012). Acute damage threshold for infrared neural stimulation of the cochlea: functional and histological evaluation. Anat Rec (Hoboken) 295:1987–1999.
33. Izzo AD, JT Walsh, Jr., ED Jansen, M Bendett, J Webb, H Ralph and CP Richter. (2007). Optical parameter variability in laser nerve stimulation: a study of pulse duration, repetition rate, and wavelength. IEEE Trans Biomed Eng 54:1108–1114.
34. Rajguru SM, AI Matic, AM Robinson, AJ Fishman, LE Moreno, A Bradley, I Vujanovic, J Breen, JD Wells, M Bendett and CP Richter. (2010). Optical cochlear implants: evaluation of surgical approach and laser parameters in cats. Hear Res 269:102–111.
35. Tome M, SL Lindsay, JS Riddell and SC Barnett. (2009). Identification of nonepithelial multipotent cells in the embryonic olfactory mucosa. Stem Cells 27:2196–2208.
36. Warchol ME, PR Lambert, BJ Goldstein, A Forge and JT Corwin. (1993). Regenerative proliferation in inner ear sensory epithelia from adult guinea pigs and humans. Science 259:1619–1622.
37. Cheng AG, LL Cunningham and EW Rubel. (2005). Mechanisms of hair cell death and protection. Curr Opin Otolaryngol Head Neck Surg 13:343–348.
38. Lim DJ. (1976). Ultrastructural cochlear changes following acoustic hyperstimulation and ototoxicity. Ann Otol Rhinol Laryngol 85:740–751.
39. Havenith S, H Versnel, MJ Agterberg, JC de Groot, RJ Sedee, W Grolman and SF Klis. (2011). Spiral ganglion cell survival after round window membrane application of brain-derived neurotrophic factor using gelfoam as carrier. Hear Res 272: 168–177.
40. Stappenbeck TS and H Miyoshi. (2009). The role of stromal stem cells in tissue regeneration and wound repair. Science 324:1666–1669.
41. Rosen AB, DJ Kelly, AJ Schuldt, J Lu, IA Potapova, SV Doronin, KJ Robichaud, RB Robinson, MR Rosen, et al. (2007). Finding fluorescent needles in the cardiac haystack: tracking human mesenchymal stem cells labeled with quantum dots for quantitative *in vivo* three-dimensional fluorescence analysis. Stem Cells 25:2128–2138.
42. Huttner WB, W Schiebler, P Greengard and P De Camilli. (1983). Synapsin I (protein I), a nerve terminal-specific phosphoprotein. III. Its association with synaptic vesicles studied in a highly purified synaptic vesicle preparation. J Cell Biol 96:1374–1388.
43. Ferreira A, HT Kao, J Feng, M Rapoport and P Greengard. (2000). Synapsin III: developmental expression, subcellular localization, and role in axon formation. J Neurosci 20:3736–3744.
44. Furness DN and DM Lawton. (2003). Comparative distribution of glutamate transporters and receptors in relation to afferent innervation density in the mammalian cochlea. J Neurosci 23:11296–11304.
45. Flores-Otero J, HZ Xue and RL Davis. (2007). Reciprocal regulation of presynaptic and postsynaptic proteins in bipolar spiral ganglion neurons by neurotrophins. J Neurosci 27:14023–14034.
46. Wang YZ, T Yamagami, Q Gan, Y Wang, T Zhao, S Hamad, P Lott, N Schnittke, JE Schwob and CJ Zhou. (2011). Canonical Wnt signaling promotes the proliferation and neurogenesis of peripheral olfactory stem cells during postnatal development and adult regeneration. J Cell Sci 124:1553–1563.
47. Ciani L and PC Salinas. (2005). WNTs in the vertebrate nervous system: from patterning to neuronal connectivity. Nat Rev Neurosci 6:351–362.
48. Ciani L, KA Boyle, E Dickins, M Sahores, D Anane, DM Lopes, AJ Gibb and PC Salinas. (2011). Wnt7a signaling promotes dendritic spine growth and synaptic strength through Ca(2)(+)/Calmodulin-dependent protein kinase II. Proc Natl Acad Sci U S A 108:10732–10737.
49. Shah SM, CH Patel, AS Feng and R Kollmar. (2013). Lithium alters the morphology of neurites regenerating from cultured adult spiral ganglion neurons. Hear Res 304:137–144.
50. Oshima K, K Shin, M Diensthuber, AW Peng, AJ Ricci and S Heller. (2010). Mechanosensitive hair cell-like cells from embryonic and induced pluripotent stem cells. Cell 141:704–716.
51. Shi F and AS Edge. (2013). Prospects for replacement of auditory neurons by stem cells. Hear Res 297:106–112.
52. Bianco P, X Cao, PS Frenette, JJ Mao, PG Robey, PJ Simmons and CY Wang. (2013). The meaning, the sense and the significance: translating the science of mesenchymal stem cells into medicine. Nat Med 19:35–42.
53. Hare JM, JE Fishman, G Gerstenblith, DL DiFede Velazquez, JP Zambrano, VY Suncion, M Tracy, E Ghersin, PV Johnston, et al. (2012). Comparison of allogeneic vs autologous bone marrow-derived mesenchymal stem cells delivered by transendocardial injection in patients with ischemic cardiomyopathy: the POSEIDON randomized trial. JAMA 308: 2369–2379.

54. Davis JA and RR Reed. (1996). Role of Olf-1 and Pax-6 transcription factors in neurodevelopment. J Neurosci 16: 5082–5094.
55. Guo Z, A Packard, RC Krolewski, MT Harris, GL Manglapus and JE Schwob. (2010). Expression of pax6 and sox2 in adult olfactory epithelium. J Comp Neurol 518:4395–4418.
56. Adamson CL, MA Reid, ZL Mo, J Bowne-English and RL Davis. (2002). Firing features and potassium channel content of murine spiral ganglion neurons vary with cochlear location. J Comp Neurol 447:331–350.
57. Matsuoka AJ, T Kondo, RT Miyamoto and E Hashino. (2007). Enhanced survival of bone-marrow-derived pluripotent stem cells in an animal model of auditory neuropathy. Laryngoscope 117:1629–1635.

Address correspondence to:
Dr. Bradley J. Goldstein
1120 NW 14th Street, 5th Floor
Miami, FL 33136

E-mail: b.goldstein4@med.miami.edu

Received for publication June 19, 2013
Accepted after revision October 29, 2013
Prepublished on Liebert Instant Online October 30, 2013